Biodegradation (2011) 22:297–307
DOI 10.1007/s10532-010-9399-z

ORIGINAL PAPER

Biodegradation of pyrene in sand, silt and clay fractions of sediment

Xinyi Cui · Wesley Hunter · Yu Yang · Yingxu Chen · Jay Gan

Received: 4 April 2010 / Accepted: 2 August 2010 / Published online: 18 August 2010

Abstract Microbial degradation is the dominant pathway for natural attenuation of PAHs in environmental compartments such as sediments, which in turn depends on the bioavailability of PAHs. The bioavailability of PAHs has seldom been studied at the sediment particle size scale. We evaluated biodegradation of pyrene by *Mycobacterium vanbaalenii* PYR-1 as a function of sediment particle sizes, and investigated the relationship between the rate of degradation on sand, silt and clay particles with their individual desorption kinetics measured with the Tenax extraction method. Regression analysis showed that the total organic carbon (TOC), black carbon (BC), and specific surface area (SSA) of the specific particle size fractions, instead of the particle size scale itself, were closely related ($P < 0.01$) with the mineralization rate. While the fraction in the rapid desorption pool (F_{rapid}) ranged from 0.11 to 0.38 for the whole sediments and different size groups, the fractions mineralized after 336-h incubation (0.52 to 0.72) greatly surpassed the F_{rapid} values, suggesting utilization of pyrene in the slow desorption pool (F_{slow}). A biodegradation model was modified by imbedding a two-phase desorption relationship describing sequential Tenax extractions. Model analysis showed that pyrene sorbed on silt and clay aggregates was directly utilized by the degrading bacteria. The enhanced bioavailability may be attributed to the higher chemical concentration, higher TOC or larger SSA in the silt and clay fractions, which appeared to overcome the reduced bioavailability of pyrene due to sorption, making pyrene on the silt and clay particles readily available to degrading microbes. This conjecture merits further investigation.

Keywords Bioavailability · Pyrene · Tenax · Particle size · Black carbon

Electronic supplementary material The online version of this article (doi:10.1007/s10532-010-9399-z) contains supplementary material, which is available to authorized users.

X. Cui (✉) · W. Hunter · Y. Yang · J. Gan
Department of Environmental Sciences, University of California, Riverside, CA 92521, USA
e-mail: lizzyc@ucr.edu

X. Cui · Y. Chen
Institute of Environmental Science and Technology, Zhejiang University, Hangzhou 310029, China

Introduction

Polycyclic aromatic hydrocarbons (PAHs) are a class of environmental organic contaminants that are of great concern due to their potency as carcinogens and mutagens. In the aquatic environment, the bed sediment usually retains most of the PAHs because of their high hydrophobicity (Kelly et al. 2007; Desai et al. 2008). Biodegradation is the key process to natural attenuation of PAHs in the environment, which in turn

depends closely on the microbial availability of PAHs sorbed on the sediment particles (Lahlou and Ortega-calvo 1999; Laor et al. 1999).

The availability of PAHs in sediment to microbes has been a subject of many studies. So far most studies examining the bioavailability of sediment-borne PAHs have considered the effect of bulk sediments and their properties, such as total organic carbon content (TOC), black carbon content (BC), specific surface areas (SSA), porosity, and aromaticity (Nam et al. 1998; Lahlou et al. 2000; Hinga 2003; Yang et al. 2009). Recognizing sediment as an assembly of different sizes of particles, a handful of researchers investigated the availability of PAHs also at the particle size scale. For instance, in suspensions, bacteria density was found to be lower on sand particles than on silt or clay particles, leading to a lower biodegradation rate of PAHs on sand (Amellal et al. 2001; Xia and Wang 2008). Talley et al. (2002), by separating a dredged sediment into coal-derived fraction and clay/silt fraction, showed that desorption and bioavailability of PAHs were more related to properties such as BC content of specific size fractions, rather than the size scale itself. However, overall, knowledge of contaminant availability at the sediment particle size scale is still scarce.

There is a point of debate about the availability of the sorbed form of chemicals in microbial degradation. Ample evidence suggests both views, i.e., microorganisms can degrade the freely dissolved form (Bouchez et al. 1995; Harms and Bosma 1997), and are also able to enhance the contaminant desorption from solid phase or directly degrade the sorbed contaminant (Guerin and Boyd 1997; Feng et al. 2000; Wick et al. 2001). A useful approach to understanding the availability of sorbed chemicals is parallel evaluation of desorption kinetics simultaneous to measurement of biodegradation (Tang et al. 1998; Park et al. 2003). Biodegradation models have been developed to take into consideration multi-phased desorption kinetics (Park et al. 2001, 2003; Beckles et al. 2007). However, the use of desorption kinetics information for evaluating bioavailability has been limited to whole sediments. In addition, extraction with Tenax beads has become a method of choice for measuring desorption kinetics due to its simplicity (e.g., Cornelissen et al. 1997; ten Hulscher et al. 2003). Consequently, there is a wealth of desorption kinetics data derived with the Tenax method. However, biodegradation models have yet to make use of such information.

The objective of this study was to evaluate factors affecting bioavailability in microbial degradation of pyrene at the sediment particle size scale. Desorption kinetics and mineralization rates were simultaneously determined for the different size fractions. A biodegradation model was modified by imbedding a two-phase desorption relationship describing sequential Tenax extractions and further tested for interpreting the role of sorption in the bioavailability of pyrene as a function of particle size.

Materials and methods

Chemicals and materials

[4, 5, 9, 10-^{14}C]Pyrene (>95% radiochemical purity; 40–60 mCi/mmol) was obtained from Sigma-Aldrich (St. Louis, MO, USA). The *Mycobacterium vanbaalenii* PYR-1 bacteria strain was donated by Dr. Cerniglia of the U.S. Food and Drug Administration in Jefferson, AR. Tenax TA® (60–80 mesh) was purchased from Supelco (Bellefonte, PA, USA). Other chemical reagents used in this study were of gas chromatography (GC) or analytical grade.

Sediment spiking and fractionation

Two freshwater sediments were used in the present study: San Diego Creek (SDC) sediment from Irvine, California, and Salinas Potrero (SP) sediment from Santa Rosa, California. The collected sediments were wet sieved through a 2-mm mesh, and stored at 4°C. The two sediments were autoclaved at 100°C for 20 min before use to remove the indigenous microbial activity. The two sterilized sediments were spiked with pyrene containing 0.05 mg/kg ^{14}C-pyrene and 0.45 mg/kg non-labeled pyrene to give an initial concentration of 0.50 mg/kg. The pyrene solution in acetone was added to the bottom of a 1.9 l wide-mouth glass jar. After the carrier solvent was removed in a fume hood, 200 g (dry wt) of sediment was added and then mixed thoroughly with a stainless steel spatula. The spiked sediments were rolled at 200 rpm for 21 d at room temperature to achieve homogenous distribution and equilibrium.

After the 21-d equilibration, the two spiked sediments were fractionated into three sizes, i.e., sand (53–2000 μm), silt (2–53 μm), and clay (<2 μm) by using a combination of wet sieving and centrifugation (Stemmer et al. 1998). Briefly, wet sediment (20 g equivalent dw) was placed in a 150-ml glass beaker and dispersed in 50 ml of deionized water using a probe type ultrasonicator (Fisher Scientific, Pittsburgh, PA, USA) with output energy of 50 J/s for 120 s. Sand was separated by manual wet sieving using a 270-mesh sieve. To purify the retained sand fraction, the sieves were rinsed once again with 200 ml deionized water. Particles remaining on the sieves were collected as the sand fraction. To separate silt particles from clay, the remaining suspension was transferred to two 200 ml centrifuge bottles and centrifuged at $150\times g$ for 5 min. The pellet after centrifuge was re-suspended with a small amount of deionized water and again centrifuged at $150\times g$ for 5 min. Particles left after centrifugation were collected as silt. All the supernatants were centrifuged at $3900\times g$ for 30 min, and the pellet after centrifugation was collected as clay.

Sediment analysis

Total organic carbon content (TOC), black (soot) carbon content (BC), specific surface areas (SSA), and pyrene concentration of the whole sediments and particle size fractions are shown in Table 1. TOC was determined by removing inorganic carbon using digestion with HCl (1 M) and analysis of the digested sample by combustion on an elemental analyzer (Flash EA1112 Soil Combustion Nitrogen/Carbon Analyzer System, Thermo Finnigan, Woods Hole, MA, USA). BC was determined following the method of Gustafsson et al. (1997). Briefly, dried and finely ground (<150 μm particle size) sediment was combusted in a muffle furnace at 375°C for 24 h. Samples were then digested with HCl (1 M) until effervescence ceased, and the BC content was then analyzed on the elemental analyzer. SSA of sediments and particle size fractions was determined by Brunauer-Emmett-Teller (BET) nitrogen isotherms using ASAP-2010 surface area analyzer (Micromeritics, Norcross, GA, USA). Concentrations of pyrene in sediment and sediment fractions were analyzed by air drying aliquots of 0.05 g (dry weight) samples in a fume hood for 24 h. The dry samples were combusted at 900°C on an OX-500 biological oxidizer (R.J. Harvey, Hillsdale, NJ, USA) for 4 min. The evolved $^{14}CO_2$ was trapped in 15 ml of Carbon-14 cocktail (R.J. Harvey) and the radioactivity was measured on a Beckman LS 5000TD liquid scintillation counter (LSC) (Fullerton, CA, USA).

Table 1 Properties of Salinas Potrero and San Diego Creek sediments and sediment fractions

	TOC (%)	BC (%)	SSA (m^2/g)	Pyrene (ng/g)
Salinas Potrero sediment				
Sediment	2.5	0.9	33.0	508.3 ± 14.9
Sand	2.8	1.1	38.0	613.5 ± 22.4
Silt	2.3	1.0	33.3	727.8 ± 14.5
Clay	2.8	0.9	45.9	376.9 ± 42.4
San Diego Creek sediment				
Sediment	0.6	0.05	3.3	409.6 ± 92.1
Sand	0.3	0	1.7	193.2 ± 38.6
Silt	2.4	0.3	21.4	1835.5 ± 50.4
Clay	3.4	1.1	43.7	826.2 ± 53.6

Biodegradation experiment

Mycobacterium vanbaalenii PYR-1, which was originally isolated from an oil-contaminated sediment, is well known for its ability to mineralize PAHs via mono- and dioxygenase reactions (Moody et al. 2002). The PYR-1 strain was cultured in 100 ml of a minimal salt medium with 1.0 g/l of pyrene as the carbon source. The strain was cultured in 250-ml Erlenmeyer flasks on a horizontal shaker at 100 rpm and 28°C for 30 d. Before the degradation kinetics tests, the bacteria cells were centrifuged at $7400\times g$ for 20 min and resuspended in the minimal salt medium to a concentration of about 10^7 cells/ml (determined on a Nanodrop ND-100 spectrophotometer (Wilmington, DE, USA)).

To determine the microbial degradation of ^{14}C-pyrene in the whole sediments and particle size fractions by the PYR-1 strain, 0.2 g (dry wt) of sample was transferred to a 40-ml amber "respirometer", followed by the addition of 2.0 ml of PYR-1 strain suspension diluted 5 times with the minimal salt medium. The setup of the respirometers was similar to a previously reported method (Doick and Semple 2003). Briefly, a 40-ml amber glass vial was attached with a 2.0 ml GC

vial filled with 1.0 ml of 1 M NaOH solution to capture the evolved $^{14}CO_2$ from mineralization of ^{14}C-pyrene. After 1, 2, 5, 24, 48, 96, 144, 192, 240 and 336 h, the NaOH solution was exchanged using 3-ml syringes, and the sample solution was mixed with 5 ml of Carbon-14 cocktail (R.J. Harvey) for measurement of radioactivity, from which the mineralization rate of ^{14}C-pyrene was calculated. Three replicates were used for each measurement. The mass balance for the degradation experiment was determined by accounting for ^{14}C associated with the residue sediment or sediment fractions after biodegradation tests and the average recovery was 86.0–103.4%.

Tenax desorption experiment

The whole sediments and particle size fractions that were used in the microbial mineralization measurement, were desorbed for different time increments using a method similar to that of Xu et al. (2008). Briefly, 1.0 g (dry wt) aliquots of sediment were transferred to 50-ml polyethylene centrifuge tubes. Tenax beads (0.05 g) and 10 ml of sodium azide solution (200 mg/l) were then added to each tube. The samples were shaken on a horizontal shaker at about 100 rpm at room temperature for 1, 2, 6, 12, 24, 48, 96, 144, 192, 240 or 336 h, with three replicates used for each desorption interval. The sample slurries were centrifuged at 1360×g for 20 min, followed by filtration of the supernatant using a Whatman No. 41 filter paper (Whatman, Maidstone, UK) to recover the Tenax beads. The trapped Tenax beads were rinsed thoroughly with deionized water and were extracted by sonication using 3 ml of acetone-hexane mixture (1:1, v/v) in 20 ml scintillation glass vials for three consecutive times. The sonication was conducted for 5 min in 2 s pulse mode with a high intensity ultrasonic processor (Sonic 550, Fisher Scientific). The extracts from the same sample were combined and mixed with 10 ml Ultima Gold LSC cocktail (Fisher Scientific), after which the ^{14}C radioactivity was measured on a Beckman LS 5000TD LSC (Fullerton, CA, USA) to derive the desorbed amount of pyrene.

The desorption kinetics up to 336 h were used to construct the desorption curve and used for estimating the initial rapid (F_{rapid}) and slow desorption fractions (F_{slow}) by fitting the data to a two-phase model (Cornelissen et al. 1997), using SigmaPlot 10.0 (San Jose, CA, USA)

$$S/S_0 = F_{rapid}e^{-k_{rapid}t} + F_{slow}e^{-k_{slow}t} \quad (1)$$

where S and S_0 (ng/g) are concentrations of pyrene in the solid phase after desorption time t (h) and before desorption, respectively, and k_{rapid} and k_{slow} are the rate constants for the rapid and slow desorption fractions, respectively.

Results and discussion

Sediment analysis

The overall recoveries of sediment mass after fractionation were 95.1 and 98.7% for SP and SDC sediments, respectively, indicating that only small quantities of sediment mass were unaccounted for after the size separation procedure. The SP sediment was dominated with the silt fraction (78.1 ± 2.0% of the total sediment mass), while for SDC sediment, 84.3 ± 3.5% of the total dry mass was sand (Fig. 1). The TOC and BC contents of the bulk SP sediment and its various size fractions were similar, with average values of 2.6 ± 0.3% and 1.0 ± 0.1%, respectively. Pronounced variations in TOC and BC contents were observed for the SDC sediment, with TOC and BC contents decreasing in the order of clay > silt > sand

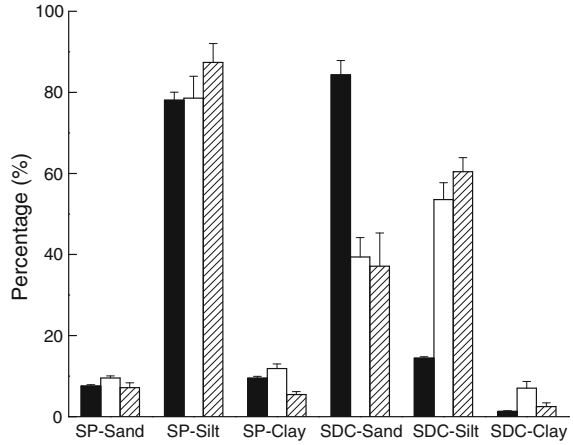

Fig. 1 Distribution of particle mass, total organic carbon content, and pyrene concentration among sand-, silt-, and clay-sized aggregates in Salinas Potrero (SP) and San Diego Creek (SDC) sediments (mass fractions: *filled bars*; TOC fractions: *blank bars*; pyrene concentration fractions: *stripped bars*)

(Table 1). In the SP sediment, the relative distribution of pyrene generally followed that of mass and TOC (Fig. 1), suggesting similar affinity of pyrene for the different sizes of particles. In contrast, although the percentage of sand mass was more than 80% in the SDC sediment, the sand fraction contained less than 40% of the total TOC or pyrene. The silt fraction, on the other hand, although accounted for only 14.5 ± 0.4% of the total mass, was associated with 53.6 ± 4.2% of the total TOC and 60.4 ± 3.5% of the total pyrene. These observations clearly suggested different affinities of TOC or pyrene for the different size aggregates of the SP sediment from the SDC sediment (Fig. 1).

Linear regression analysis was performed for all the samples across two sediments, and the results showed that there was a poor correlation between pyrene distribution and mass fractions of the sediments ($r^2 = 0.69$; $P = 0.15$). However, the relative distribution of pyrene among the three size fractions was found to closely correlate with TOC in those fractions ($r^2 = 0.99$; $P < 0.01$), as well as with BC contents ($r^2 = 0.84$; $P < 0.05$). This observation was consistent with the conclusion of Oen et al. (2006), and suggested that distribution of PAHs among the different sediment size particles was mainly driven by organic carbon.

Biodegradation of pyrene as function of particle sizes

Biodegradation of pyrene in the two sediments and their particle size fractions was rapid and progressed without an apparent acclimation phase (Figs. 2, 3). For the SP sediment, mineralization of pyrene followed similar trends among the different particle size fractions. After 336 h of incubation, the percentages of pyrene mineralized by *Mycobacterium vanbaalenii* PYR-1 were not significantly different among the sand (51.73 ± 8.95%), silt (55.11 ± 2.25%), and clay (55.92 ± 2.83%) fractions (Fig. 2a). For the SDC sediment, mineralization of pyrene appeared to be faster in the sand fraction than in the silt or clay fraction (72.27 ± 14.27% in sand fraction versus 63.38 ± 3.78% and 59.42 ± 4.92% in silt and clay fractions, Fig. 3a). The sum of cumulative mineralization from the different size fractions, calculated after mass normalization over the specific size fractions, closely approximated the mineralization measured independently from the whole sediment for both

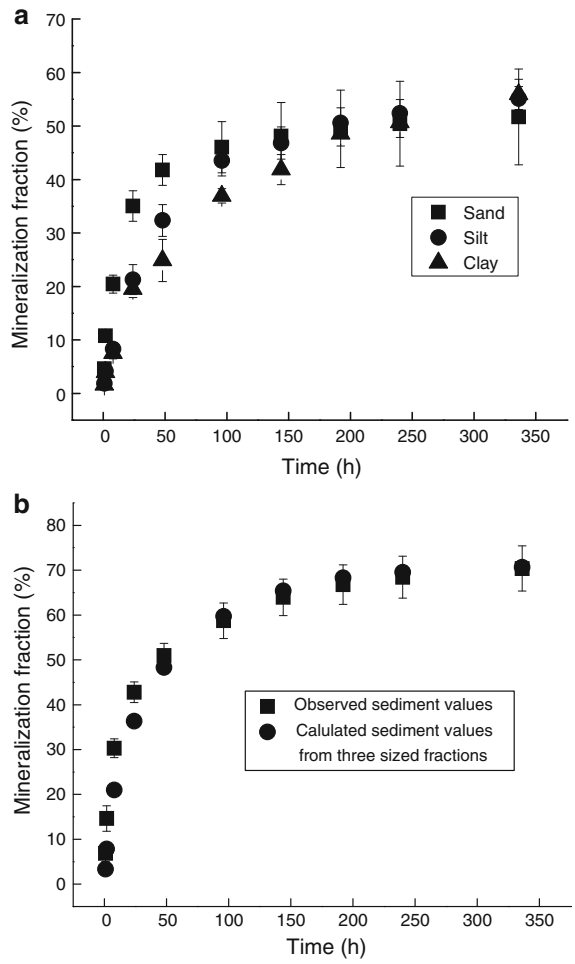

Fig. 2 Pyrene degradation kinetics up to 336 h by the PYR-1 strain in SP sediment. **a** Mineralization in the sediment size aggregates: sand-(*filled square*), silt-(*filled circle*), and clay-sized (*filled triangle*) aggregates. **b** Observed mineralization values in the whole sediment particles (*filled square*) and the calculated values from the three sized fractions (*filled circle*) Bars represent standard deviations ($n = 3$)

sediments (Figs. 2b, 3b), suggesting the rigorousness of measurement and also that the physical separation of sediment aggregates did not modify the original availability of pyrene for microbial degradation.

Studies using whole sediments show that sediment organic matter quantity and quality are the most important variables affecting the microbial availability of PAHs in sediments (Nam et al. 1998; Lahlou and Ortega-calvo 1999). Some studies also suggest that other sediment properties, including the SSA, may influence microbial degradation of PAHs (Lahlou et al. 2000; Xia and Wang 2008). After combining all the

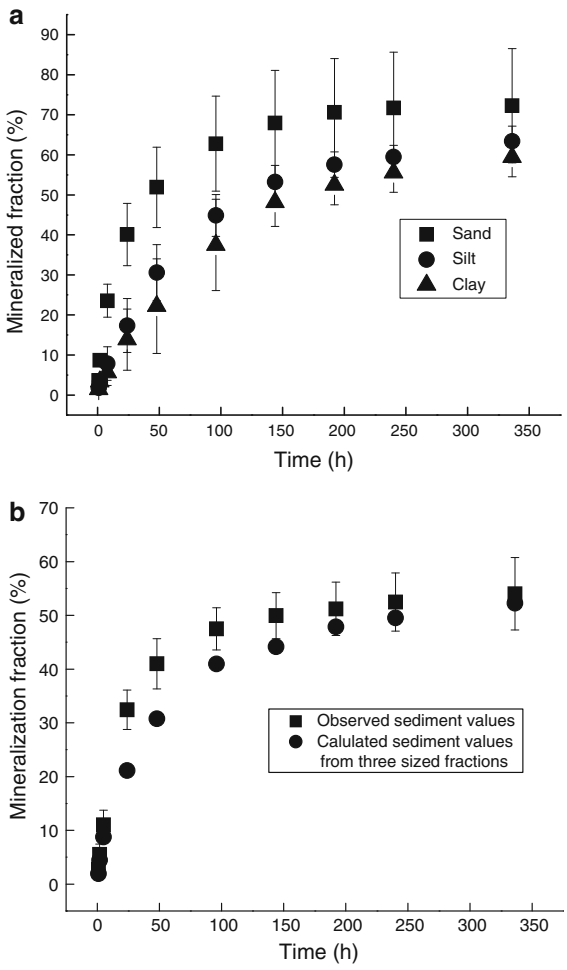

Fig. 3 Pyrene degradation kinetics up to 336 h by the PYR-1 strain in SDC sediment. **a** Mineralization in the sediment size aggregates: sand-(*filled square*), silt-(*filled circle*), and clay-sized (*filled triangle*) aggregates. **b** Observed mineralization values in the whole sediment particles (*filled square*) and the calculated values from the three sized fractions (*filled circle*) Bars represent standard deviations ($n = 3$)

size fractions from the two sediments, linear correlation analysis between the mineralized fractions after 336 h and the selected sediment particle properties showed a good correlation for TOC ($r = -0.84$, $P < 0.01$), BC ($r = -0.94$, $P < 0.001$) and SSA ($r = -0.89$, $P < 0.01$). It is noteworthy that the r values between mineralization and TOC, BC, and SSA were all negative, suggesting a negative effect of these properties on pyrene availability. The overall analysis showed that the microbial availability of pyrene from the different size fractions was independent of particle sizes, but was closely influenced by the associated particle properties, including especially BC content.

Desorption kinetics of pyrene as a function of particle sizes

The desorption kinetics of pyrene was measured for the whole sediments and their particle size fractions. The desorption kinetics fitted well to the two-phase desorption model with $r^2 \geq 0.97$ (Fig. 4; Table 2). Linear correlation analysis showed that in general, there was a lack of relationship between the sizes of desorption pools (F_{rapid} and F_{slow}) and the selected particle properties including TOC and BC (The value of P ranged from 0.062 to 0.65). In earlier studies, differences in desorption of hydrophobic organic compounds (HOCs) were also found to be poorly related to specific sediment properties (Cornelissen et al. 1999; Kukkonen et al. 2003).

Several studies suggested that F_{rapid} reflected the pool of contaminant attached to the outer regions of sediment aggregates and may be used as an indicator for the bioaccessible fraction of sediment- or soil-associated HOCs (Cornelissen et al. 1998; You et al. 2006). However, in this study F_{rapid} ranged from 0.11 to 0.38 for the two sediments and their particle size fractions (Table 2), which were substantially smaller than the mineralized fractions after 336 h (51.73–55.92% and 59.42–72.27% for SP and SDC sediments, Figs. 2, 3). Therefore, the pyrene-degrading bacteria clearly accessed and utilized some of the pyrene in the F_{slow} pool. This finding was in agreement with several previous studies where the researchers also demonstrated the availability of desorption-resistant fractions during microbial degradation (Lahlou and Ortega-calvo 1999; Huesemann et al. 2004; Lee et al. 2009).

In order to further determine if pyrene in F_{slow} was bioavailable, a biodegradation model that takes into account the contribution to mineralization by F_{slow} was used to fit biodegradation kinetic data in the current study (Lahlou and Ortega-calvo 1999).

$$P = v_2 t + (v_1 + v_2)(1 - e^{-kt})/k \quad (2)$$

where P is percentage of biodegradation fraction of pyrene as a function of time, t(h), v_1 represents the initial rate of biodegradation (%/h), v_2 is the rate of biodegradation resulting from F_{slow} (%/h), and k is

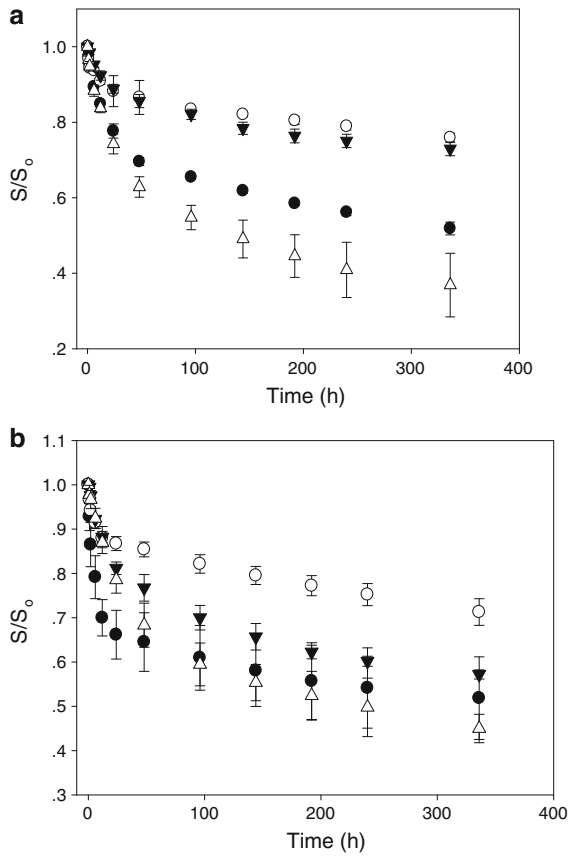

Fig. 4 Desorption kinetics of pyrene from SP (**a**) and SDC (**b**) sediment (*filled circle*), and different size fractions, sand (*open circle*), silt (*filled inverted triangle*), and clay (*open triangle*). S/S_0 is the ratio of chemical concentration remaining in the sediment after desorption time t to that present in the sediment before desorption, and t is the cumulative desorption time

the first-order rate constant (1/h). All the v_2 values estimated from the model were significantly higher than 0, and were 0.77–8.6% of the corresponding v_1 values (Supporting information, Table S1). Given that F_{slow} is often much larger than F_{rapid}, this suggests a significant contribution from the slowly desorbing pool.

Model analysis of microbial availability of pyrene

A coupled model considering both desorption and biodegradation was used to analyze the biodegradation results of ^{14}C-pyrene in the sediment fractions. An assumption used in the coupled model was that the degrading bacteria utilized only liquid-phase substrate. The biodegradation of a substrate in a closed system containing solid particles and water may be expressed as (Feng et al. 2000; Park et al. 2001, 2003; Beckles et al. 2007):

$$V\frac{\partial C}{\partial t} + m\frac{\partial S}{\partial t} = -\mu CV \tag{3}$$

where V is the volume of the solution (ml), m is the mass of solid (g), t is time (h), C is the aqueous concentration (ng/ml), S is the chemical concentration remaining in the sediment phase (ng/g), and μ is the first-order biodegradation rate constant (1/h) in the solution phase. The microbial mineralization rate in the solution phase (μ) was determined to be 0.126 (1/h) through preliminary experiments using sediment-free samples under conditions similar to the sediment

Table 2 Mean regression parameters from fitting Tenax desorption data of pyrene in sediments or sediment fractions to a two-phase desorption model[a]

Treatment	F_{rapid}	k_{rapid} (1/h)	F_{slow}	k_{slow} (1/h)	r^2
Salinas Potrero sediment					
Sediment	0.29 ± 0.01	5.17 ± 0.67 ($\times 10^{-2}$)	0.70 ± 0.01	$8.68 \times 10^{-4} \pm 6.82 \times 10^{-5}$	0.99
Sand	0.11 ± 0.02	7.75 ± 0.32 ($\times 10^{-2}$)	0.87 ± 0.01	$4.06 \times 10^{-4} \pm 4.62 \times 10^{-6}$	0.99
Silt	0.15 ± 0.01	$4.26 \times 10^{-2} \pm 7.18 \times 10^{-3}$	0.84 ± 0.01	$4.57 \times 10^{-4} \pm 5.10 \times 10^{-5}$	0.99
Clay	0.38 ± 0.02	$3.56 \times 10^{-2} \pm 4.74 \times 10^{-3}$	0.60 ± 0.02	$1.45 \times 10^{-3} \pm 1.41 \times 10^{-5}$	0.97
San Diego Creek sediment					
Sediment	0.31 ± 0.03	$1.79 \times 10^{-1} \pm 4.15 \times 10^{-2}$	0.67 ± 0.02	$7.90 \times 10^{-4} \pm 1.21 \times 10^{-4}$	0.98
Sand	0.11 ± 0.02	$2.35 \times 10^{-1} \pm 7.41 \times 10^{-2}$	0.88 ± 0.01	$6.19 \times 10^{-4} \pm 4.46 \times 10^{-5}$	0.99
Silt	0.26 ± 0.02	$4.65 \times 10^{-2} \pm 1.12 \times 10^{-2}$	0.74 ± 0.02	$7.67 \times 10^{-4} \pm 1.03 \times 10^{-4}$	0.99
Clay	0.35 ± 0.01	$3.22 \times 10^{-2} \pm 1.10 \times 10^{-3}$	0.64 ± 0.01	$1.05 \times 10^{-3} \pm 2.48 \times 10^{-5}$	0.98

[a] F_{rapid} and F_{slow} are the rapid and slow desorption fractions, respectively, and k_{rapid} and k_{slow} are the corresponding rate constants

slurry treatments. When combined with the Tenax-aided desorption model (Eq. 1), Eq. 3 becomes:

$$V\frac{\partial C}{\partial t} + \mu CV = mS_0(F_{\text{rapid}}k_{\text{rapid}}e^{-k_{\text{rapid}}t} + F_{\text{slow}}k_{\text{slow}}e^{-k_{\text{slow}}t}) \quad (4)$$

Equation 4 can be solved numerically to an integration form that depicts the change of aqueous-phase concentration C with time:

$$C = \frac{\text{mS}_0F_{rapid}k_{\text{rapid}}}{V(\mu - k_{\text{rapid}})}e^{-k_{\text{rapid}}t} + \frac{mS_0F_{\text{slow}}k_{\text{slow}}}{V(\mu - k_{\text{slow}})}e^{-k_{\text{slow}}t} \quad (5)$$

The mineralized amount of pyrene was calculated based on the change of C during the incubation time. Mineralization rates were estimated using the desorption-biodegradation coupled model (Eq. 5, model 1) to evaluate pyrene bioavailability in sample slurries. If only dissolved pyrene in the bulk-aqueous phase was degraded, the amount of pyrene mineralized should equal to the model prediction. In contrast, mineralization rates exceeding the predicted values would imply enhanced bioavailability. An upper boundary of the model estimate would be the assumption of instantaneous desorption, where $F_{\text{slow}} = 0$ and Eq. (5) is simplified to Eq. (6) (model 2):

$$C = \frac{\text{mF}_{\text{rapid}}\text{S}_0k_{\text{rapid}}}{V(\mu - k_{\text{rapid}})}e^{-k_{\text{rapid}}t} \quad (6)$$

For the SP sediment, the measured mineralization curves for all of the three particle size fractions fell above the predicted line by model 1 (Fig. 5), indicating that the bacteria not only utilized pyrene in the solution phase, but also either enhanced the desorption of pyrene into the solution phase or directly used the sorbed pyrene. The measured mineralization curve for the sand aggregates fell between model 1 and model 2 predicted lines. In comparison, the measured mineralization for the silt fraction closely mimicked the model 2 prediction while that for the clay fraction clearly surpassed that predicted by the model 2 in the later phase of the incubation experiment (Fig. 5). Similar patterns were also observed for the SDC sediment (Fig. 6). Again, while the measured mineralization fell between the two predicted lines for the sand fraction, the cumulative mineralization was similar to that predicted by the model 2 for silt, and was greater than that predicted by the model 2 for clay (Fig. 6). The increased mineralization in relation to that predicted by the model 2 implied that pyrene sorbed on silt and clay particles was probably used directly by the PYR-1 bacteria, that is, without first being desorbed into the solution phase.

Direct utilization of sorbed form of compounds by the degrading bacteria has also been observed in a few earlier studies (Feng et al. 2000; Park et al. 2003; Huesemann et al. 2004; Lee et al. 2009; Yang et al. 2009), even though in these studies the microbial availability was not considered at the particle size scale. The enhanced availability of pyrene to the PAH degrading bacteria on silt and clay fractions as opposed to the sand fraction in our study may be attributed to properties specific to these particle sizes. For bacteria, it is known that the properties of chemotaxis towards the substrate facilitate the bacteria's access to the surface of solid particles that have elevated chemical concentrations (Van Loosdrecht et al. 1990; Leglize et al. 2008), and a positive relationship between atrazine concentrations and access to the pool of sorbed atrazine was previously observed in Park et al. (2003). Marx and Aitken (2000) reported that inoculated bacteria moved to certain places where more naphthalene was available, leading to an enhanced biodegradation of naphthalene. In Amellal et al. (2001), the transmission electron microscopy observations showed that the bacteria were most numerous on fine silt and clay aggregates, where the highest concentration of PAHs were located. In the current study, the concentration of pyrene in the silt fraction was higher than that in the sand or clay fractions, especially for the SDC sediment. Although not measured directly in this study, it is probable that more bacteria moved and became attached onto the surface of the silt particles as compared to the other particle sizes, resulting in relatively higher utilization of pyrene sorbed on the silt particles.

Two factors that have been shown to affect the sorption of bacteria to solid particles are SSA and TOC (Xia and Wang 2008). Lahlou et al. (2000) demonstrated that clay, which has relatively larger SSA, was the most important retarding compartment for both hydrophobic and nonhydrophobic PAH-degrading bacteria. Bogan and Sullican (2003) further demonstrated that PAH-degrading bacteria tended to bind to organic matter of solid particles. In this study, SSA of the silt- and clay-sized particles

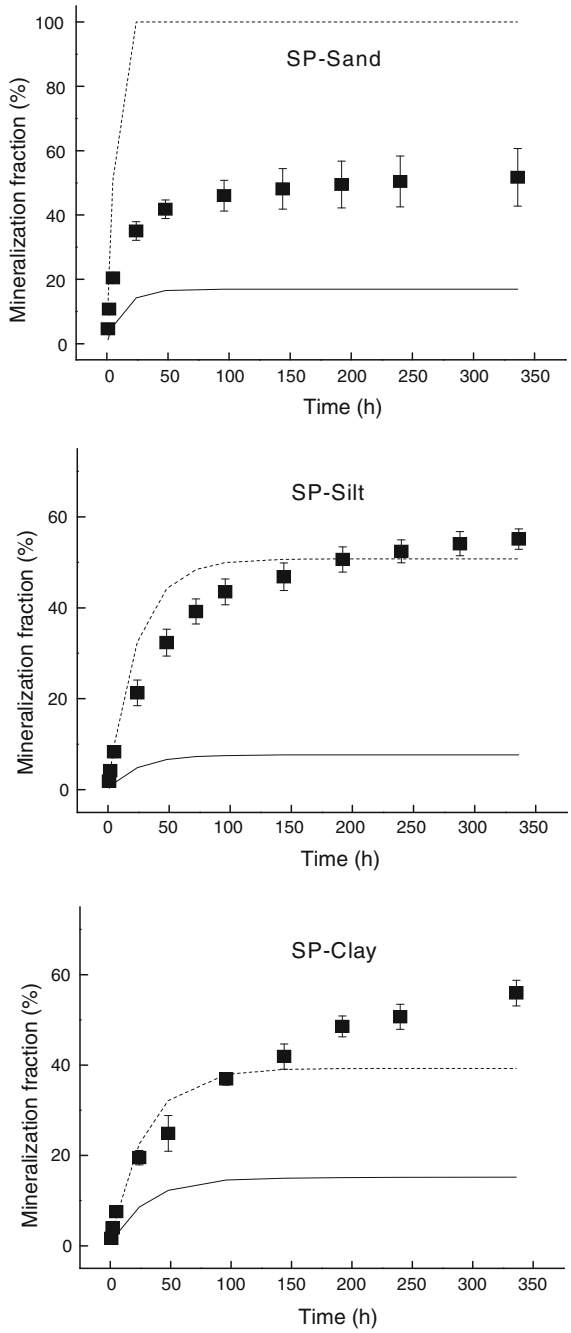

Fig. 5 Microbial mineralization of pyrene (*filled square*: observed values) on various sized particles in SP sediment. The solid lines represent the model 1 predicted values, and the dash lines represent the model 2 predicted values

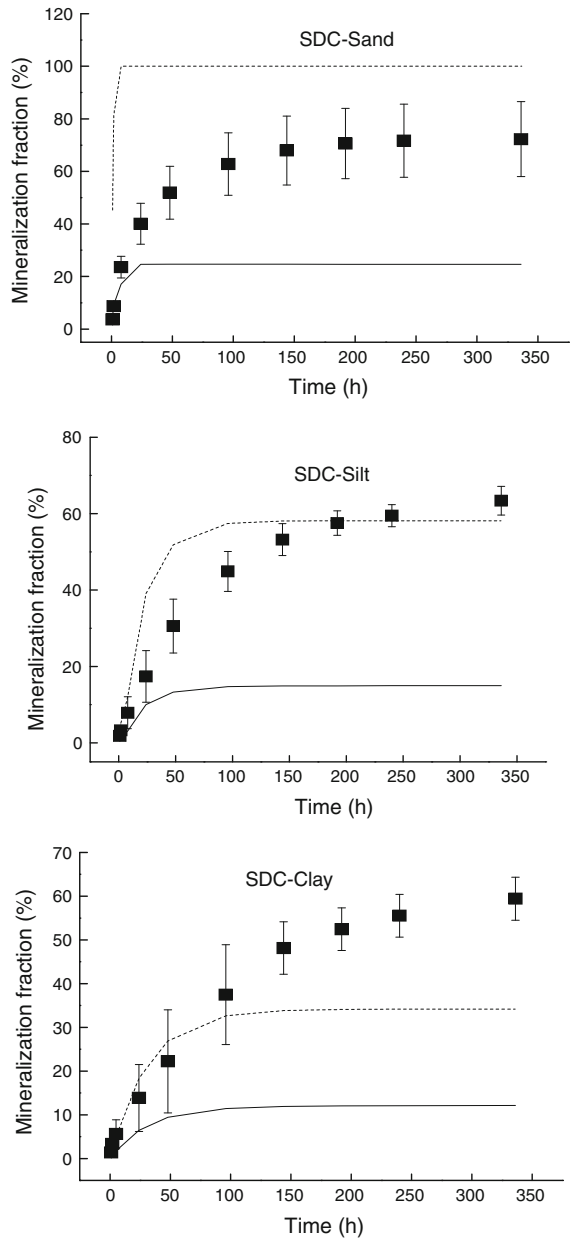

Fig. 6 Microbial mineralization of pyrene (*filled square*: observed values) on various sized particles in SDC sediment. The solid lines represent the model 1 predicted values, and the dash lines represent the model 2 predicted values

was larger than the sand fraction, especially for the SDC sediment. For instance, SSA of clay and silt from the SDC sediment was 25.4 and 12.4 fold that of sand particles (Table 1). Therefore, the silt and clay fractions could provide more sites for bacteria to attach, likely leading to a higher direct utilization of sorbed pyrene. In addition, the clay fractions of the two sediments had the highest TOC contents as compared to the other fractions. Therefore, more

bacteria could have moved to the clay fractions than to the other fractions containing less TOC, contributing to a further enhanced utilization and biodegradation of pyrene sorbed to the clay aggregate.

References

Amellal N, Portal JM, Vogel T, Berthelin J (2001) Distribution and location of polycyclic aromatic hydrocarbons (PAHs) and PAH-degrading bacteria within polluted soil aggregates. Biodegradation 12:49–57

Beckles DM, Chen W, Hughes JB (2007) Bioavailability of polycylic aromatic hydrocarbons sequestered in sediment: microbial study and model prediction. Environ Toxicol Chem 26:878–883

Bogan BW, Sullican WR (2003) Physicochemical soil parameters affecting sequestration and mycobacterial biodegradation of polycyclic aromatic hydrocarbons in soil. Chemosphere 52:1717–1726

Bouchez M, Blanchet D, Vandecasteele JP (1995) Substrate availability in phenanthrene biodegradation: transfer mechanism and influence on metabolism. Appl Microbiol Biotechnol 43:952–960

Cornelissen G, van Noort PCM, Govers HAJ (1997) Desorption kinetics of chlorobenzenes, polycyclic aromatic hydrocarbons, and polychlorinated biphenyls: sediment extraction with Tenax and effects of contact time and solute hydrophobicity. Environ Toxicol Chem 16:1351–1357

Cornelissen G, Rigterink H, Ferdinandy MMA, van Noort PCM (1998) Rapidly desorbing fractions of PAHs in contaminated sediments as a predictor of the extent of bioremediation. Environ Sci Technol 32:966–970

Cornelissen G, van Zuilen H, van Noort PCM (1999) Particle size dependence of slow desorption of in situ PAHs from sediments. Chemosphere 38:2369–2380

Desai AM, Autenrieth RL, Dimitriou-Christidis P, McDonald TJ (2008) Biodegradation kinetics of select polycyclic aromatic hydrocarbon (PAH) mixtures by *Sphingomonas paucimobilis* EPA505. Biodegradation 19:223–233

Doick KJ, Semple KT (2003) The effect of soil: water ratios on the mineralisation of phenanthrene: LNAPL mixtures in soil. FEMS Microb Lett 220:29–33

Feng YC, Park JH, Voice TC, Boyd SA (2000) Bioavailability of soil-sorbed biphenyl to bacteria. Environ Sci Technol 34:1977–1984

Guerin WF, Boyd SA (1997) Bioavailability of naphthalene associated with natural and synthetic sorbents. Water Res 31:1504–1512

Gustafsson Ö, Haghseta F, Chan C, MacFarlane J, Gschwend PM (1997) Quantification of the dilute sedimentary soot phase: implications for PAH speciation and bioavailability. Environ Sci Technol 31:203–209

Harms H, Bosma TNP (1997) Mass transfer limitation of microbial growth and pollutant degradation. J Ind Microbiol Biotechnol 18:97–105

Hinga KR (2003) Degradation rates of low molecular weight PAH correlate with sediment TOC in marine subtidal sediment. Mar Pollut Bull 46:466–474

Huesemann MH, Hausmann TS, Fortman TJ (2004) Does bioavailability limit biodegradation? A comparison of hydrocarbon biodegradation and desorption rates in aged soils. Biodegradation 15:261–274

Kelly BC, Ikonomou MG, Blair JD, Morin AE, Gobas FAPC (2007) Food web-specific biomagnification of persistent organic pollutants. Science 317:236–239

Kukkonen JVK, Landrum PF, Mitra S, Gossiaux DC, Gunnarson J, Weston D (2003) Sediment characteristics affecting desorption kinetics of select PAH and PCB congeners for seven laboratory spiked sediments. Environ Sci Technol 37:4656–4663

Lahlou M, Ortega-calvo JJ (1999) Bioavailability of labile and desorption-resistant phenanthrene sorbed to montmorillonite clay containing humic fractions. Environ Toxicol Chem 18:2729–2735

Lahlou M, Harms H, Springael D, Ortega-Calvo JJ (2000) Influence of soil components on the transport of polycyclic aromatic hydrocarbon-degrading bacteria through saturated porous media. Environ Sci Technol 34:3649–3656

Laor Y, Strom PF, Farmer WJ (1999) Bioavailability of phenanthrene sorbed to mineral-associated humic acid. Wat Res 33:1719–1729

Lee SJ, Pardue JH, Moe WM, Kim DJ (2009) Effect of sorption and desorption-resistance on biodegradation of chlorobenzene in two wetland soils. J Hazard Mater 161:492–498

Leglize P, Saada A, Berthelin J, Leyval C (2008) Adsorption of phenanthrene on activated carbon increases mineralization rate by specific bacteria. J Hazard Mater 151:339–347

Marx RB, Aitken MD (2000) Bacterial chemotaxis enhances naphthalene degradation in a heterogeneous aqueous system. Environ Sci Technol 34:3379–3383

Moody JD, Doerge DR, Freeman JP, Cerniglia CE (2002) Degradation of biphenyl by Mycobacterium sp. strain PYR-1. Appl Microbiol Biotechnol 58:364–369

Nam K, Chung N, Alexander M (1998) Relationship between organic matter content of soil and the sequestration of phenanthrene. Environ Sci Technol 32:3785–3788

Oen AMP, Cornelissen G, Breedveld GD (2006) Relation between PAH and black carbon contents in size fractions of Norwegian harbor sediments. Environ Pollut 141:370–380

Park JH, Zhao XD, Voice TC (2001) Biodegradation of non-desorbable naphthalene in soils. Environ Sci Technol 35:2734–2740

Park JH, Feng YC, Ji PS, Voice TC, Boyd SA (2003) Assessment of bioavailability of soil-sorbed atrazine. Appl Environ Microbiol 69:3288–3298

Stemmer M, Gerzabeki MH, Kandeler E (1998) Organic matter and enzyme activity in particle-size fractions of soils obtained after low-energy sonication. Soil Biol Biochem 30:9–17

Talley JW, Gosh U, Tucker SG, Furey JS, Luthy RG (2002) Particle-scale understanding of the bioavailability of PAHs in sediment. Environ Sci Technol 36:477–483

Tang WC, White JC, Alexander M (1998) Utilization of sorbed compounds by microorganisms specifically isolated for that purpose. Appl Microbiol Biotechnol 49:117–121

ten Hulscher TEM, Postma J, den Besten PJ, Stroomberg GJ, Belfroid A, Wegener JW, Faber JH, van der Pol JJC, Hendriks AJ, van Noort PCM (2003) Tenax extraction mimics benthic and terrestrial bioavailability of organic compounds. Environ Toxicol Chem 22:2258–2265

Van Loosdrecht MCM, Lyklema J, Norde W, Zehnder AJB (1990) Influence of interfaces on microbial activity. Microbiol Rev 54:75–87

Wick LY, Colangelo T, Harms H (2001) Kinetics of mass transfer limited bacterial growth on solid PAHs. Environ Sci Technol 35:354–361

Xia X, Wang R (2008) Effect of sediment particle size on polycylic aromatic hydrocarbon biodegradation: Importance of the sediment-water interface. Environ Toxicol Chem 27:119–125

Xu YP, Gan J, Wang ZJ, Spurlock F (2008) Effect of aging on desorption kinetics of sediment-associated pyrethroids. Environ Toxicol Chem 27:1293–1301

Yang Y, Hunter W, Tao S, Gan J (2009) Microbial availability of different forms of phenanthrene in soils. Environ Sci Technol 43:1852–1857

You J, Landrum PF, Lydy MJ (2006) Comparison of chemical approaches for assessing bioavailability of sediment-associated contaminants. Environ Sci Technol 40:6348–6353